Spins and parities of the odd-A P isotopes within a relativistic mean-field model and elastic magnetic electron-scattering theory

Zaijun Wang,[1,*] Zhongzhou Ren,[2,3] Tiekuang Dong,[4] and Chang Xu[2]
[1]*School of Science, Tianjin University of Technology and Education, Tianjin 300222, China*
[2]*Department of Physics, Nanjing University, Nanjing 210008, China*
[3]*Center of Theoretical Nuclear Physics, National Laboratory of Heavy-Ion Accelerator at Lanzhou, Lanzhou 730000, China*
[4]*Purple Mountain Observatory, Chinese Academy of Sciences, Nanjing 210008, China*
(Received 18 March 2014; revised manuscript received 21 June 2014; published 11 August 2014)

The ground-state spins and parities of the odd-A phosphorus isotopes $^{25-47}$P are studied with the relativistic mean-field (RMF) model and relativistic elastic magnetic electron-scattering theory (REMES). Results of the RMF model with the NL-SH, TM2, and NL3 parameters show that the $2s_{1/2}$ and $1d_{3/2}$ proton level inversion may occur for the neutron-rich isotopes $^{37-47}$P, and, consequently, the possible spin-parity values of $^{37-47}$P may be $\frac{3}{2}^+$, which, except for ^{47}P, differs from those given by the NUBASE2012 nuclear data table by Audi *et al.* Calculations of the elastic magnetic electron scattering of $^{37-47}$P with the single valence proton in the $2s_{1/2}$ and $1d_{3/2}$ state show that the form factors have significant differences. The results imply that elastic magnetic electron scattering can be a possible way to study the $2s_{1/2}$ and $1d_{3/2}$ level inversion and the spin-parity values of $^{37-47}$P. The results can also provide new tests as to what extent the RMF model, along with its various parameter sets, is valid for describing the nuclear structures. In addition, the contributions of the upper and lower components of the Dirac four-spinors to the form factors and the isotopic shifts of the magnetic form factors are discussed.

DOI: 10.1103/PhysRevC.90.024307 PACS number(s): 21.10.Pc, 21.10.Hw, 25.30.Bf, 21.60.Cs

I. INTRODUCTION

Spin and parity are two of the fundamental properties of nuclei. Spin-parity values are in most cases necessary for studying nuclear processes and other nuclear properties. Measuring the spin-parity values of stable and long-lived nuclei is not a problem at present, and the spins and parities of nearly all stable and long-lived nuclei have been determined experimentally [1]. However, for most of the short-lived nuclei, measurement of nuclear spins and parities is still very difficult. The spin-parity values of the short-lived nuclei given in the NUBASE2012 nuclear data table [1] are mostly estimated from trends in neighboring nuclides (TNN) with the same parities in N and Z.

In view of the shell theory, most of the nucleon spins and orbital momenta in a nucleus pair off to produce zero contribution to the whole nucleus. Thus nuclear spins and parities are just determined by several valence nucleons [2–6]. Since the magnetic moment of a nucleus is closely related to its spin, we can obtain information about nuclear spins and parities by studying the electromagnetic interaction processes involving nuclei. One of the most widely used processes is magnetic electron-nucleus scattering. The magnetic electron-nucleus scattering process has its own advantage and uniqueness in studying the nuclear structures due to its sensitivity to the states of motion of the valence nucleons [2–11], whether they are protons or neutrons, because both the protons and neutrons have intrinsic magnetic moments. Thus, we expect that the magnetic electron-nucleus scattering can provide information on the nuclear spins and parities. As a matter of fact, as early as 1983, such an idea was already put forward by J. Heisenberg and H. P. Blok [12]. They discussed how it is possible to determine the spin and parity values of some of the excited states of several stable even-even nuclei. In the past, electron-nucleus scattering already provided a great deal of information on the electromagnetic properties of stable and long-lived nuclei. Nowadays, in order to use this excellent probe to study the structures of short-lived nuclei, based on the development of radioactive-isotope- (RI) beam technology, some new facilities for electron scattering off short-lived nuclei have been constructed or under construction at different laboratories. The MUSES and self-confining radioactive isotope ion target [13–16] at RIKEN in Japan has been constructed and the "First Demonstration of Electron Scattering Using a Novel Target Developed for Short-Lived Nuclei" with stable nucleus ^{133}Cs was already performed in 2009 [17,18]. The Electron-Ion Scattering in a Storage Ring project, which was designed to scatter electrons with an energy of 125–500 MeV and to perform elastic, inelastic, and quasielastic electron scattering off short-lived radioactive isotopes at the Facility for Antiproton and Ion Research (now under construction) at GSI in Germany [19], has also been planned. Moreover, great progress in parity-violating electron-nucleus scattering with high precision has also been achieved recently at the Thomas Jefferson National Accelerator Facility in the United States [20,21]. Therefore, it is expected that, with the development of nuclear experimental technologies, electron scattering on short-lived nuclei will be realized in the near future.

In parallel with the construction of the new-generation electron-scattering facilities, theoretical studies of electron scattering on unstable nuclei have also started [22–33]. These studies are mainly concerned with the Coulomb electron scattering and parity-violating electron scattering. They have studied different possible responses of the electron-scattering observables to the exotic structures of unstable nuclei, such as

*zjwang@tute.edu.cn

the halo structure, and have provided many useful references for the possible future experimental work. Inspired by the idea of Ref. [12], in this paper, we would like to study how the elastic magnetic electron-scattering form factors response to the change of spins and parities of some unstable odd-A nuclei. For this purpose, we choose to perform theoretical investigations on the odd-A phosphors isotopes. The odd-A phosphorus isotopes have 15 protons and an even number of neutrons, so, according to the shell theory, their $1s$, $1p$ proton shells and the $1d_{5/2}$ proton subshell should be fully occupied by 14 protons and thus the ground-state spins and parities are determined only by a single valence proton outside the $1d_{5/2}$ orbital. Another reason why we chose the odd-A phosphorus isotopes is that these nuclei are in the s-d shell region, where the order of the $2s_{1/2}$ and $1d_{3/2}$ proton energy levels is predicted to be more likely to invert with an increasing excess of neutrons. Moreover, the experimental data of the magnetic form factors, the charge from factors, the root-mean-square radius of the electric charge distribution, and the magnetic moment of ^{31}P are all available [2,34–37]. These experimental data can provide very good opportunities for comparisons of theoretical results. Therefore, the odd-A phosphorus isotopes are ideal for theoretical calculations.

The theory that we use in the present research is the combination of the relativistic mean-field model (RMF) and the elastic magnetic electron-scattering theory in the relativistic frame. The RMF model has been extensively used to describe the properties of the ground and low excited states of both stable and unstable nuclei [38–49], so we combine this theory with the elastic magnetic electron-scattering theory to fulfill our study. We use the RMF model, along with the NL-SH [43], NL3 [45], and TM2 [48] parameter sets, to investigate the energy level structures and produce the single-nucleon wave functions. Taking the wave functions as inputs, we can calculate the magnetic form factors with the elastic magnetic electron-scattering theory. The results of the RMF model and the elastic magnetic electron-scattering theory are discussed in detail. We expect to carry out an investigation into the effects that the neutron excess can has on the spins and parities of these nuclei and find out if it is possible for the elastic magnetic electron scattering to be used for probing them. In addition, we also expect that the present study can provide some new references for testing to what extent the RMF model is valid for describing the unstable nuclei.

The paper is organized in the following way. Section II is the formalism of elastic magnetic electron scattering in the relativistic frame. Section III is the numerical results and discussions. A summary is given in Sec. IV.

II. FORMALISM

In the relativistic frame, the single-particle wave functions [50] can be expressed as follows:

$$\psi_{n\kappa m} = \begin{bmatrix} i\,[G(r)/r]\,\Phi_{\kappa m}(\hat{r}) \\ -[F(r)/r]\,\Phi_{-\kappa m}(\hat{r}) \end{bmatrix} = \begin{bmatrix} i|n\kappa m\rangle \\ -\overline{|n\kappa m\rangle} \end{bmatrix} = \begin{bmatrix} i\left|nl\,\frac{1}{2}\,jm\right\rangle \\ -\left|nl^{'}\,\frac{1}{2}\,jm\right\rangle \end{bmatrix}. \tag{1}$$

With the choice of the phase factor in Eq. (1), the upper and lower components $G(r)$ and $F(r)$ are real functions. The orbital and the total angular-momentum quantum numbers l, $l^{'}$, and j are uniquely determined by the angular quantum number κ [38], where

$$j = |\kappa| - \tfrac{1}{2}, \tag{2}$$

with

$$l = \kappa, \quad l^{'} = l - 1, \quad (\kappa > 0), \tag{3}$$

$$l = -(\kappa + 1), \quad l^{'} = l + 1, \quad (\kappa < 0), \tag{4}$$

and the functions $\Phi_{\kappa m}$ in Eq. (1) are the spinor spherical harmonics,

$$\Phi_{\kappa m} = \sum_{m_l m_s} \left\langle l m_l \tfrac{1}{2} m_s \middle| l\,\tfrac{1}{2}\,jm \right\rangle Y_{lm_l}\chi_{m_s}. \tag{5}$$

In the shell model of nuclear structure, only the unpaired valence nucleon contributes to the magnetic form factors. With the magnetic multipole operator $\hat{T}^{\rm mag}_{LM}(q)$, the elastic magnetic form factors squared can be written as

$$F^2_M(q) = \frac{4\pi f^2_{\rm sn}(q) f^2_{\rm c.m.}(q)}{2J_i + 1} \sum_{L=1}^{\rm odd} \left|\langle J_f|\left|\hat{T}^{\rm mag}_L\right||J_i\rangle\right|^2, \tag{6}$$

where the multipole operator is defined by [2,51,52]

$$\hat{T}^{\rm mag}_{LM}(q) = \int j_L(qr)\boldsymbol{Y}^M_{LL}(\hat{r}) \cdot \hat{J}(\boldsymbol{r}) d^3\boldsymbol{r} \tag{7}$$

and

$$\langle J_f M_f|\hat{T}^{\rm mag}_{LM}(q)|J_i M_i\rangle = (-)^{J_f - M_f} \begin{pmatrix} J_f & J & J_i \\ -M_f & M & M_i \end{pmatrix} \times \langle J_f|\left|\hat{T}^{\rm mag}_L(q)\right||J_i\rangle, \tag{8}$$

and the single-nucleon factor and center-of-mass (c.m.) factor in Eq. (6) are given by $f_{\rm sn}(q) = [1 + (q/855\,{\rm MeV})^2]^{-2}$ and $f_{\rm c.m.}(q) = \exp(q^2b^2/4A)$, respectively. Here, b is the oscillator parameter, which is commonly taken as $b = A^{1/6}{\rm fm}^{-1}$; q is the momentum transfer and $\boldsymbol{Y}^M_{LL}(\hat{r})$ is the vector spherical harmonics [53].

With the formulas given by Refs. [38,54,55], Eq. (6) can be further expressed as

$$F^2_M(q) = \frac{4\pi f^2_{\rm sn}(q) f^2_{\rm c.m.}(q)}{2J_i + 1} \sum_{L=1}^{\rm odd} \left|R^u_L(q) + R^l_L(q) + R^c_L(q)\right|^2, \tag{9}$$

where

$$R^u_L(q) = -(q/2M_n)(\langle n\kappa\|\lambda^{'}\Sigma^{'M}_L\|n\kappa\rangle, \tag{10}$$

$$R^l_L(q) = (q/2M_n)\overline{\langle n\kappa\|}\lambda^{'}\Sigma^{'M}_L\overline{\|n\kappa\rangle}, \tag{11}$$

$$R^c_L(q) = 2\overline{\langle n\kappa\|}Q\Sigma^M_L\|n,\kappa\rangle. \tag{12}$$

The $R^u_L(q)$, $R^l_L(q)$, and $R^c_L(q)$ denote the contributions of the upper and the lower components of the Dirac four-spinors and the crossed term, respectively. In Eqs. (10)–(12), the Q, M_n, and $\lambda^{'}$ are the electric charge, mass, and magnetic moment of

the nucleon, respectively, and the operators Σ_L^M and $\Sigma_L^{'M}$ are given by [38,54,55]

$$\Sigma_L^M(\boldsymbol{r}) \equiv \boldsymbol{M}_{LL}^M(\boldsymbol{r}) \cdot \boldsymbol{\sigma}, \quad \Sigma_L^{'M}(\boldsymbol{r}) \equiv -i\left(\nabla \times \boldsymbol{M}_{LL}^M(\boldsymbol{r})\right) \cdot \boldsymbol{\sigma}/q, \quad \boldsymbol{M}_{LL}^M(\boldsymbol{r}) \equiv j_L(qr)\boldsymbol{Y}_{LL}^M(\hat{r}).$$

The single-particle reduced matrix elements in Eqs. (10)–(12) can be calculated with the formulas given by Edmonds [53] and Willey [56]. By partial integration, the reduced matrix elements can be expressed explicitly as follows:

$$\begin{aligned}\langle n\kappa \| \Sigma_L^{'M} \| n\kappa \rangle = {} & \frac{(-1)^{l+1}}{q}\left(\frac{6}{4\pi}\right)^{1/2}(2l+1)(2j+1) \\ & \times \left[\begin{Bmatrix} l & l & L+1 \\ \frac{1}{2} & \frac{1}{2} & 1 \\ j & j & L \end{Bmatrix} \begin{pmatrix} l & L+1 & l \\ 0 & 0 & 0 \end{pmatrix} (L(2L+3))^{1/2} \times \int dr r^2 j_L(qr)\left(\frac{d}{dr} + \frac{L+2}{r}\right) g^2(r) \right. \\ & \left. + \begin{Bmatrix} l & l & L-1 \\ \frac{1}{2} & \frac{1}{2} & 1 \\ j & j & L \end{Bmatrix} \begin{pmatrix} l & L-1 & l \\ 0 & 0 & 0 \end{pmatrix} ((L+1)(2L-1))^{1/2} \times \int dr r^2 j_L(qr)\left(\frac{d}{dr} - \frac{L-1}{r}\right) g^2(r) \right], \end{aligned} \tag{13}$$

$$\begin{aligned}\overline{\langle n\kappa \| \Sigma_L^{'M} \| n\kappa \rangle} = {} & \frac{(-1)^{l'+1}}{q}\left(\frac{6}{4\pi}\right)^{1/2}(2l'+1)(2j+1) \times \left[\begin{Bmatrix} l' & l' & L+1 \\ \frac{1}{2} & \frac{1}{2} & 1 \\ j & j & L \end{Bmatrix} \begin{pmatrix} l' & L+1 & l' \\ 0 & 0 & 0 \end{pmatrix} (L(2L+3))^{1/2} \right. \\ & \times \int dr r^2 j_L(qr)\left(\frac{d}{dr} + \frac{L+2}{r}\right) f^2(r) + \begin{Bmatrix} l' & l' & L-1 \\ \frac{1}{2} & \frac{1}{2} & 1 \\ j & j & L \end{Bmatrix} \begin{pmatrix} l' & L-1 & l' \\ 0 & 0 & 0 \end{pmatrix} ((L+1)(2L-1))^{1/2} \\ & \left. \times \int dr r^2 j_L(qr)\left(\frac{d}{dr} - \frac{L-1}{r}\right) f^2(r) \right], \end{aligned} \tag{14}$$

and

$$\overline{\langle n\kappa \| \Sigma_L^M \| n\kappa \rangle} = (-1)^{l'}\left(\frac{6}{4\pi}\right)^{1/2}(2L+1)(2j+1)((2l+1)(2l'+1))^{1/2} \begin{Bmatrix} l' & l & L \\ \frac{1}{2} & \frac{1}{2} & 1 \\ j & j & L \end{Bmatrix} \begin{pmatrix} l' & L & l \\ 0 & 0 & 0 \end{pmatrix} \int dr r^2 j_L(qr) g(r) f(r), \tag{15}$$

where $g(r) = G(r)/r$, $f(r) = F(r)/r$.

To calculate the magnetic form factors, we also need a reliable nuclear structure model to produce the single-nucleon wave functions. We use the RMF model to generate the wave functions $g(r) = G(r)/r$ and $f(r) = F(r)/r$. Since the details of the RMF model can be found in many articles, such as Refs. [38–49], we will not repeat them here.

III. NUMERICAL RESULTS AND DISCUSSIONS

A. The results of the relativistic mean-field model

In this section, we present the results of the odd-A $^{25-47}$P calculated by using the RMF model with the NL-SH, TM2, and NL3 force parameters.

In Table I, we list the binding energies per nucleon E/A (MeV) and the root-mean-square (rms) charge radii $R_{\rm rms}$ (fm) of $^{25-47}$P, as well as the results given by the NUBASE2012 nuclear data table [1]. Detailed examination on the results in Table I shows that for each isotope the discrepancies of E/A and $R_{\rm rms}$ among the theoretical results and between the theoretical and experimental results are all very small. For the binding energies per nucleon, the discrepancies among the results given by the three sets of parameters are less than 0.18 MeV (<2.19%), and those between the theoretical results and the experimental ones are less than 0.16 MeV (<2.33%). For the root-mean-square charge radii, the differences among the results given by the three sets of parameters are less than 0.079 fm (<2.38%). For ^{31}P, whose charge radius experimental data are available (3.191(5) fm [35], 3.19(3) fm [36], and 3.187 fm [36]), the discrepancies of $R_{\rm rms}$ between the theoretical results and the experimental ones are less than 0.047 fm (<1.47%). These results, from one aspect, show that the RMF model is reliable in describing the phosphorus isotopes.

To know how to implement the calculation of the magnetic form factors, we need to make a detailed analysis on the structure of the s-d proton shell for the considered nuclei. In Table II, we present the $1d_{5/2}$, $2s_{1/2}$, and $1d_{3/2}$ single-proton energy levels $\varepsilon(1d_{5/2})$ (MeV), $\varepsilon(2s_{1/2})$ (MeV), and $\varepsilon(1d_{3/2})$ (MeV) and the proton occupation probabilities of the $1d_{5/2}$ orbital $p(1d_{5/2})$. In Fig. 1, we also present the variations of the $1d_{3/2}$-$1d_{5/2}$ spin-orbit splitting gap $\Delta\varepsilon = \varepsilon(1d_{3/2}) - \varepsilon(1d_{5/2})$ [Fig. 1(b)], along with the occupation probabilities of the $1d_{5/2}$ orbital [Fig. 1(a)], with respect to the neutron number.

It can be seen from Table II that for $^{25-35}$P the three parameter sets all predict that the $2s_{1/2}$ energy levels are lower than the $1d_{3/2}$ levels. While for ^{37}P and ^{39}P, the predictions appear to differ. The NL3 predicts that the $2s_{1/2}$ levels are lower than the $1d_{3/2}$ ones, whereas NL-SH and TM2 predict

TABLE I. The theoretical results of the binding energies per nucleon and the root-mean-square charge radii of $^{25-47}$P, as well as the binding energies per nucleon given in the NUBASE2012 nuclear data table.

	NL-SH		TM2		NL3		NUBASE2012
	E/A	$R_{\rm rms}$	E/A	$R_{\rm rms}$	E/A	$R_{\rm rms}$	E/A
^{25}P	6.832	3.296	6.971	3.375	6.852	3.312	6.812#
^{27}P	7.559	3.204	7.719	3.274	7.563	3.215	7.663
^{29}P	8.151	3.153	8.320	3.219	8.141	3.160	8.251
^{31}P	8.325	3.166	8.442	3.234	8.353	3.170	8.481
^{33}P	8.417	3.190	8.488	3.259	8.442	3.199	8.514
^{35}P	8.461	3.214	8.494	3.285	8.475	3.227	8.446
^{37}P	8.283	3.223	8.333	3.300	8.292	3.242	8.268
^{39}P	8.083	3.242	8.146	3.315	8.081	3.257	8.099
^{41}P	7.900	3.259	7.969	3.332	7.886	3.273	7.907
^{43}P	7.695	3.276	7.782	3.349	7.691	3.289	7.690
^{45}P	7.473	3.291	7.538	3.365	7.478	3.304	7.470#
^{47}P	7.237	3.306	7.293	3.380	7.269	3.317	7.200#

that the $2s_{1/2}$ levels are higher than the $1d_{3/2}$ ones. This shows that $2s_{1/2}$ and $1d_{3/2}$ level inversion in ^{37}P and ^{39}P may exist. For $^{41-47}$P, the predictions of the three sets of parameters again agree with one another, but they all show that the $2s_{1/2}$ and $1d_{3/2}$ level inversion may occur to $^{41-47}$P. The predictions of the three parameter sets for $^{25-47}$P are not exactly the same; nevertheless, they still have two important features in common. One is that the general trends of the $2s_{1/2}$ and $1d_{3/2}$ levels are similar. The other is that they all predict that the $2s_{1/2}$ and $1d_{3/2}$ proton level inversion may exist in the neutron-rich phosphorus isotopes. The second feature reveals that the neutron excess can have significant influence on the states of motion of the protons near the Fermi surface.

In addition to the $2s_{1/2}$ and $1d_{3/2}$ proton level inversion, the neutron excess may also have influence on the proton occupation probability of the $1d_{5/2}$ orbital, since the $1d_{3/2}$-$1d_{5/2}$ spin-orbit splitting gap will get narrowed with the increase of the neutron number and the $1d_{5/2}$ proton orbital is near the Fermi surface for the P isotopes. The results of $1d_{5/2}$ and $1d_{3/2}$ in Table II and the variations of the splitting gap in Fig. 1(b) indicate that for $^{25-47}$P the splitting gap indeed gradually narrows with an increasing neutron number. However, as the results show that for the very neutron rich isotopes, such as ^{47}P, the spin-orbit splitting gap is around 6.6 MeV, which is about 2 times larger than the pairing gaps of $^{25-47}$P, which are around 1.63–2.24 MeV according to

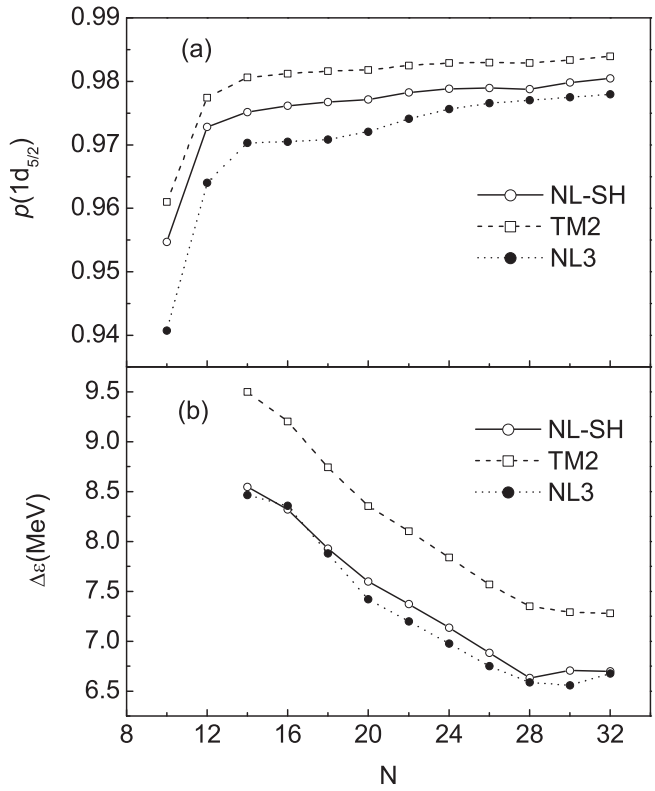

FIG. 1. The proton occupation probabilities of the $1d_{5/2}$ orbital (a) and the $1d_{3/2}$-$1d_{5/2}$ spin-orbit splitting gaps (b) calculated with NL-SH, TM2, and NL3 parameters.

TABLE II. The $1d_{5/2}$, $2s_{1/2}$, and $1d_{3/2}$ single-proton energy levels and the occupation probabilities of the $1d_{5/2}$ orbital of $^{25-47}$P calculated with the NL-SH, TM2, and NL3 parameters.

	NL-SH				TM2				NL3			
	$\varepsilon(1d_{5/2})$	$\varepsilon(2s_{1/2})$	$\varepsilon(1d_{3/2})$	$p(1d_{5/2})$	$\varepsilon(1d_{5/2})$	$\varepsilon(2s_{1/2})$	$\varepsilon(1d_{3/2})$	$p(1d_{5/2})$	$\varepsilon(1d_{5/2})$	$\varepsilon(2s_{1/2})$	$\varepsilon(1d_{3/2})$	$p(1d_{5/2})$
^{25}P	−4.441	−0.231	Unbound	0.9547	−4.761	−0.018	Unbound	0.9610	−4.256	−0.995	Unbound	0.9408
^{27}P	−7.588	−1.725	Unbound	0.9728	−7.956	−1.359	Unbound	0.9774	−7.391	−2.539	Unbound	0.9641
^{29}P	−10.601	−3.392	−2.054	0.9752	−11.041	−2.878	−1.543	0.9806	−10.444	−4.209	−1.978	0.9703
^{31}P	−12.922	−5.728	−4.602	0.9761	−13.301	−5.182	−4.101	0.9812	−12.619	−6.859	−4.261	0.9705
^{33}P	−15.201	−7.895	−7.272	0.9767	−15.584	−7.346	−6.841	0.9816	−14.809	−8.996	−6.928	0.9709
^{35}P	−17.392	−9.997	−9.794	0.9772	−17.763	−9.441	−9.409	0.9818	−16.955	−10.793	−9.533	0.9721
^{37}P	−19.565	−11.826	−12.192	0.9782	−19.856	−11.196	−11.755	0.9825	−18.955	−12.474	−11.756	0.9741
^{39}P	−21.677	−13.553	−14.543	0.9788	−21.957	−12.865	−14.118	0.9829	−20.924	−14.085	−13.948	0.9757
^{41}P	−23.716	−15.216	−16.834	0.9790	−23.958	−14.468	−16.390	0.9829	−22.788	−15.633	−16.037	0.9765
^{43}P	−25.687	−16.828	−19.055	0.9788	−25.619	−15.930	−18.270	0.9829	−24.338	−17.074	−17.750	0.9770
^{45}P	−25.961	−17.763	−19.257	0.9798	−26.453	−17.095	−19.162	0.9834	−25.342	−18.362	−18.783	0.9775
^{47}P	−26.675	−18.800	−19.976	0.9804	−27.097	−18.127	−19.818	0.9839	−26.260	−19.493	−19.583	0.9780

$\Delta = 11.2/\sqrt{A}$ MeV, so the pair scattering of the protons from the $1d_{5/2}$ orbital to the $1d_{3/2}$ orbital is not strong for these nuclei. Likewise, for the same reason, the pair scattering from the $1d_{5/2}$ orbital to $2s_{1/2}$ orbital is also not strong. Therefore, the proton occupation probability of the $1d_{5/2}$ orbital should be nearly unaffected by the change of the spin-orbit splitting gap. Figure 1(a) is the variation of the proton occupation probabilities of $1d_{5/2}$ with respect to the neutron number. It shows that with the increase of the neutron number the proton occupation probability of the $1d_{5/2}$ orbital has a very slow increase from 0.94 to 0.98. Therefore, it would be a good approximation to assume that the $1d_{5/2}$ proton orbital maintains fully occupied when calculating the magnetic form factors of $^{25-47}$P.

It is known that a particle prefers to move in a lower energy state, so the inversion of the $2s_{1/2}$ and $1d_{3/2}$ energy levels will change the proton occupancy of the two states in $^{37-47}$P and, consequently, may lead to the change of the spin-parity values of these nuclei. Based on the results in Table II and the nuclear shell theory, we can obtain the ground-state spin-parity values of $^{25-47}$P predicted by the RMF model with the three sets of parameters. The results, along with those given by NUBASE2012 (the rightmost column), are listed in Table III. It would be very interesting to make a detailed comparison among the results given in the table. It can be found from the table that for the isotopes $^{25-35}$P, among which the spin-parity values of $^{27-35}$P are determined, the results given by the three sets of parameters not only agree with one another but also agree with those given by NUBASE2012. For the other isotopes, whose spin-parity values are unknown at present, the predicted results are mostly not agree with those given by NUBASE2012. For ^{37}P and ^{39}P, the spins and parities predicted by the NL3 parameters are $\frac{1}{2}^+$, which agrees with those given by NUBASE2012, whereas the results of both nuclei predicted by NL-SH and TM2 are $\frac{3}{2}^+$, otherwise $\frac{1}{2}^+$. For $^{41-45}$P, the three parameter sets all give $\frac{3}{2}^+$, and they do not agree with the values given by NUBASE2012. For ^{47}P, the three parameter sets and NUBASE2012 all give the same result, $\frac{3}{2}^+$.

TABLE III. The spin-parity values of $^{25-47}$P predicted by the RMF model and those given by NUBASE2012. The symbol # in the table indicates that the values are estimated from trends in neighboring nuclides with the same Z and N parities.

	NL-SH	TM2	NL3	NUBASE2012
^{25}P	$\frac{1}{2}^+$	$\frac{1}{2}^+$	$\frac{1}{2}^+$	$\frac{1}{2}^+$#
^{27}P	$\frac{1}{2}^+$	$\frac{1}{2}^+$	$\frac{1}{2}^+$	$\frac{1}{2}^+$
^{29}P	$\frac{1}{2}^+$	$\frac{1}{2}^+$	$\frac{1}{2}^+$	$\frac{1}{2}^+$
^{31}P	$\frac{1}{2}^+$	$\frac{1}{2}^+$	$\frac{1}{2}^+$	$\frac{1}{2}^+$
^{33}P	$\frac{1}{2}^+$	$\frac{1}{2}^+$	$\frac{1}{2}^+$	$\frac{1}{2}^+$
^{35}P	$\frac{1}{2}^+$	$\frac{1}{2}^+$	$\frac{1}{2}^+$	$\frac{1}{2}^+$
^{37}P	$\frac{3}{2}^+$	$\frac{3}{2}^+$	$\frac{1}{2}^+$	$\frac{1}{2}^+$#
^{39}P	$\frac{3}{2}^+$	$\frac{3}{2}^+$	$\frac{1}{2}^+$	$\frac{1}{2}^+$#
^{41}P	$\frac{3}{2}^+$	$\frac{3}{2}^+$	$\frac{3}{2}^+$	$\frac{1}{2}^+$#
^{43}P	$\frac{3}{2}^+$	$\frac{3}{2}^+$	$\frac{3}{2}^+$	$\frac{1}{2}^+$#
^{45}P	$\frac{3}{2}^+$	$\frac{3}{2}^+$	$\frac{3}{2}^+$	$\frac{1}{2}^+$#
^{47}P	$\frac{3}{2}^+$	$\frac{3}{2}^+$	$\frac{3}{2}^+$	$\frac{3}{2}^+$#

We can draw some important information from the above comparisons. First, the result that the spin-parity values obtained with the three sets of parameters and from experiments for all those isotopes ($^{27-35}$P) whose spin-parity values have been determined by experiments all agree with one another shows that, to a great extent, the RMF model is stable and reliable for calculating the properties of the considered nuclei. Then the difference between the results given by NL-SH and TM2 and those given by NL3 for ^{37}P and ^{39}P reveal that there also exist some uncertainties in predicting nuclear properties with the RMF model. This difference may indicate that different sets of parameters dwell at places with different distances to the reality; one set may be better than the others. Usually, it is very difficult to determine which parameter set or sets is better just based on the specific values given by the RMF model, since, in most cases, for a specific nucleus the single-nucleon energy levels, the total binding energies or the binding energies per nucleon, and the charge radii calculated with different sets of parameters do not have substantial discrepancies. However, this difference is substantial and may provide another reference to help us determine which set or sets of parameters is better. Moreover, the agreement of the predicted spin-parity values of ^{47}P with one another and with that given by NUBASE2012 seems to strongly suggest that it is very likely that there exists $2s_{1/2}$ and $1d_{3/2}$ level inversion in ^{47}P. Finally, it can be found naturally from the comparison that, in theory, the odd-A phosphorus isotopes are really a group of very good candidate nuclei for investigating the $2s_{1/2}$ and $1d_{3/2}$ level inversion and for studying the validity of the RMF model, along with its various sets of parameters, for unstable nuclei. The rich and diversified results of the odd-A phosphorus isotopes given by the RMF model with the three parameter sets, and the agreement and disagreement among the theoretical results and those given by NUBASE2012, can offer good opportunities for us to make comparisons with the results from experiments and other theories. These discussions suggest that if we can find an experimental method to determine the states of motion of the single valence proton in $^{37-47}$P, we can not only know the spins and parities of these nuclei but also learn more about the long-debated nuclear level inversion and the validity of the RMF nuclear structure theory.

B. The results of the elastic magnetic electron-scattering theory

The discussions of the previous section show that the single valence proton in $^{37-47}$P may move in the $1d_{3/2}$ orbital or the $2s_{1/2}$ orbital due to the possible $2s_{1/2}$ and $1d_{3/2}$ proton level inversion. Does the level inversion in $^{37-47}$P really exist? Which of the two states does the single valence proton really move in? The answers to both problems concern not only the existence of the $2s_{1/2}$ and $1d_{3/2}$ level inversion and the spin-parity values of $^{37-47}$P but also the validity of the RMF model for unstable nuclei. Elastic magnetic electron scattering is an excellent tool for investigating the states of motion of the valence nucleons in nuclei, especially the states of motion of a single valence nucleon outside a closed

shell or a fully occupied subshell in an odd-A nucleus. The odd-A isotopes $^{25-47}$P are such nuclei, with a single valence proton moving outside the $1d_{5/2}$ orbital. In this section, we present investigations of $^{25-47}$P with the elastic magnetic electron-scattering theory in the relativistic frame. We examine the responses of the magnetic form factors to the two states of motion of the single valence proton in these nuclei and explore if elastic magnetic electron scattering is feasible for investigating the $2s_{1/2}$ and $1d_{3/2}$ proton level inversion and determining the spins and parities of $^{37-47}$P experimentally.

Before the calculation of the form factors of $^{25-47}$P, we need to further test the reliability of the single-nucleon wave functions given by the RMF model. To this end, we choose to calculate the form factors of odd-A ^{31}P and ^{29}Si and compare the results with the experimental data. In theoretical calculations of magnetic electron-nucleus scattering, it is very common that the many-body effects, such as those of the meson exchange and back flow currents in the relativistic mean field, are considered by introducing the spectroscopy factors α_L to the scattering multipoles. In practice, the first spectroscopy factor α_1 is usually chosen to be the ratio of the experimental nuclear magnetic moment to the single-nucleon value $\mu_{\rm exp}/\mu_{\rm sn}$, because of the lack of experimental data in the very low momentum transfer region, where M_1 dominates the magnetic scattering. For ^{31}P, there is only the M_1 multipole, so we take the factor $\alpha_1 = 1.131/2.793$, where 1.131 μ_N is the experimental value [37] of the magnetic moment of ^{31}P. Likewise, for ^{29}Si, there is only one valence neutron in the $2s_{1/2}$ orbital, so we take the spectroscopy factor $\alpha_1 = -0.55529/(-1.913)$, where -0.55529 μ_N is the experimental value [37] of the magnetic moment of ^{29}Si. The results of both nuclei are presented in Fig. 2. These results are obtained directly from the single-nucleon wave functions generated by the RMF model. Except the spectroscopy factor α_1, no other corrections or adjustments are made. The figure shows that there exist some slight discrepancies between the theoretical form factors and the experimental ones for both nuclei. The discrepancies appear around the second maximum for ^{31}P and some slightly larger discrepancies occur on both sides of the minimum for ^{29}Si. In addition, the form factors given by different parameter sets also show some slight deviations. Even so, the theoretical form factors for both nuclei agree well on a large part with the experimental data [2,34]. This shows that the wave functions generated by the RMF model are, to a great extent, reliable. This, on the other hand, also confirms the rationality of introducing the first spectroscopy factor by choosing $\alpha_1 = \mu_{\rm exp}/\mu_{\rm sn}$. More examples for testing the reliability of the RMF model can also be found in Ref. [57]. Based on these results, we assume that the single-nucleon wave functions produced by the RMF model are reliable. Under this assumption, we can only consider the single-nucleon contributions to the magnetic scattering in the following calculations. We make such an assumption for two reasons. One is that our purpose is to see if the elastic magnetic electron scattering is sensitive to the states of motion of the single valence nucleon and how it responses to the changes of the states of motion of the valence nucleon. The other is that we do not have enough experimental data to fit for the spectroscopy factors of $^{25-47}$P.

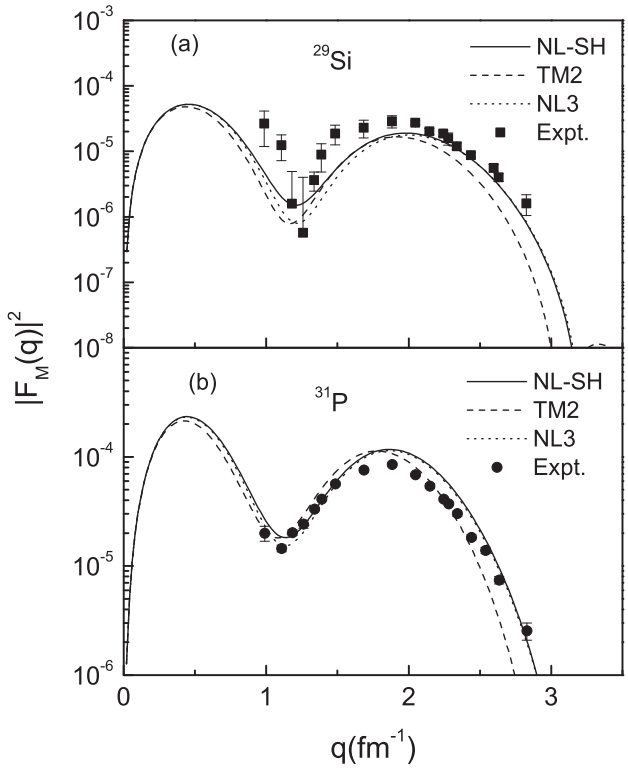

FIG. 2. Comparisons of the theoretical magnetic form factors of ^{31}P and ^{29}Si with the experimental data [2,34].

For clearness, we divide the isotopes $^{25-47}$P into two groups according to the results in Tables II and III in the following calculations. For the parameter sets NL-SH and TM2, the first group includes $^{25-35}$P, and the second group consists of $^{37-47}$P. For the parameter set NL3, the first group includes $^{25-39}$P; the second group, $^{41-47}$P. For the two first groups, since the RMF model predictions for the spin-parity values of $^{27-35}$P all agree with the experimental results and indicate no level inversion of the $2s_{1/2}$ and $1d_{3/2}$ states, we assume that the single valence proton in these nuclei moves in the $2s_{1/2}$ orbital. Taking the wave functions generated by the RMF model as input, we can calculate the elastic magnetic form factors of $^{25-39}$P. The numerical results are presented in Fig. 3. The figure shows that the trends of variation of the form factors given by the three sets of force parameters are very similar, but there appears to be a noticeable isotopic shift for each parameter set. Within the most easily measured momentum transfer region $q = 0.5$–3.0 fm^{-1}, the greatest form factor shifts between the isotopes occur around the first minimum near $q = 1.0$ fm^{-1}. These shifts, which tend to become nonsignificant with the increase of the neutron number, reveal the changes of the wave functions of the single valence proton under the influence of an increasing neutron number. This result shows that the appropriate momentum transfer region to measure the isotopic shifts of the magnetic form factors of $^{25-37}$P is around $q = 1.0$ fm^{-1}.

For the second group, since the RMF model calculations show that there may exist $2s_{1/2}$ and $1d_{3/2}$ level inversion, we calculate the magnetic form factors in two cases. In one case, we assume that the valence proton moves in the $2s_{1/2}$ orbital;

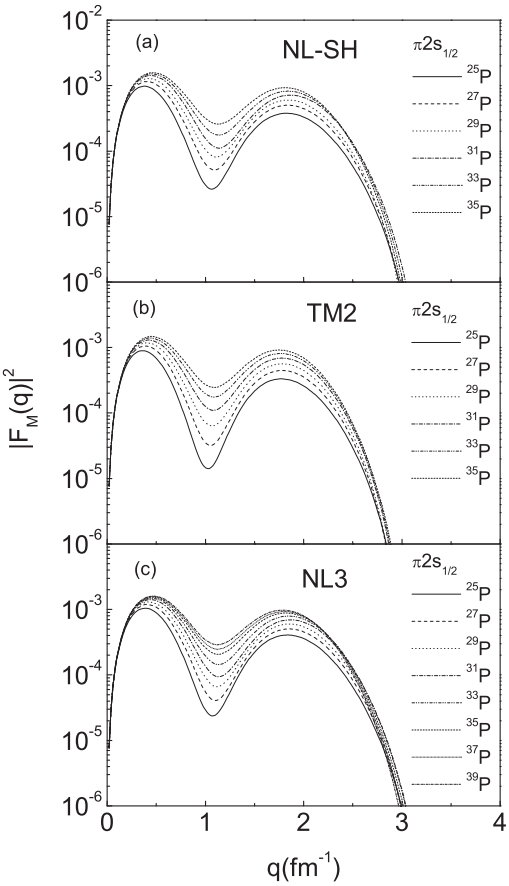

FIG. 3. The magnetic form factors of $^{25-35}$P calculated with the NL-SH and TM2 parameter sets and those of $^{25-39}$P calculated with NL3 parameter set. In the figure, $\pi 2s_{1/2}$ denotes that the valence proton is in the $2s_{1/2}$ orbital.

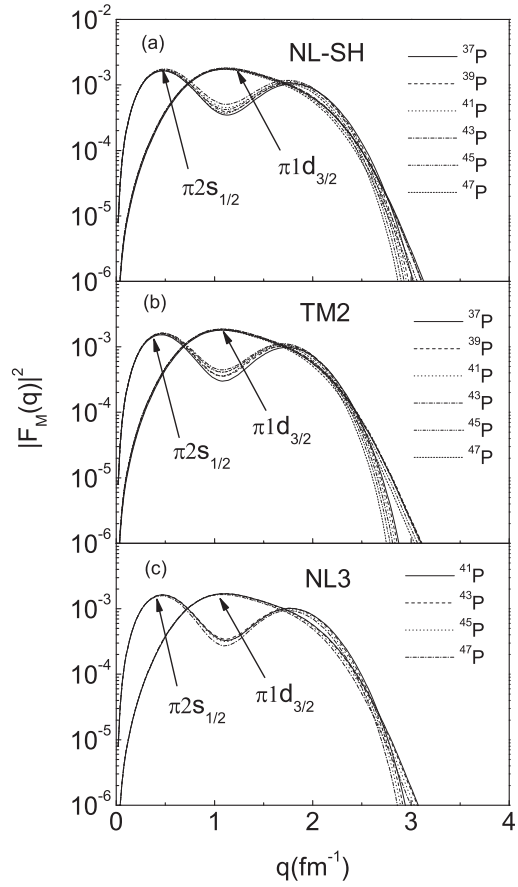

FIG. 4. The same as Fig. 3 but for the isotopes $^{37-47}$P. In the figure, $\pi 2s_{1/2}$ and $\pi 1d_{3/2}$ denote that the single valence proton is in the $2s_{1/2}$ and $1d_{3/2}$ orbitals, respectively.

in another, the valence proton occupies the $1d_{3/2}$ orbital. The results are presented in Fig. 4. In the figure, $\pi 2s_{1/2}$ and $\pi 1d_{3/2}$ denote that the valence proton is in the $2s_{1/2}$ and $1d_{3/2}$ orbitals, respectively. The curves in the figure show three features. First, for either case the trends of variation of the magnetic form factors are very similar. This again shows that the RMF model is stable. Second, unlike the form factors shown in Fig. 3, for the very neutron rich isotopes $^{37-47}$P, the increase of the neutron number only makes a small difference to the form factors in the momentum transfer region near $q = 1.0$ fm^{-1}, and only very slight shifts of the form factors appear in the momentum transfer region $q = 0.5$–3.0 fm^{-1}. Third, the form factors of $^{37-47}$P in the two cases show significant differences, especially in the region $q = 0$–2.0 fm^{-1}. Both the shapes and the trends of variation of the form factors differ remarkably with each other. The third feature is of great significance. It implies that the two different states of motion of the valence proton can have significantly different influences on the magnetic form factors or on the magnetic moment distributions of these nuclei. This significant difference indicates that the state of motion of the single valence proton in $^{37-47}$P can probably be probed experimentally with elastic magnetic electron scattering.

Based on the above results, it can be concluded theoretically that elastic magnetic electron scattering might be a feasible way for experimental study of the spins and parities of $^{37-47}$P. With the development and application of the new-generation electron-nucleus collider at Riken and GSI, it is expected that the magnetic form factors of the short-lived nuclei can be measured in the future. Then the present theoretical results can be used as references for determining the possible *s*-*d* level inversion and the spins and parities and for testing to what extent the RMF model, along with its various sets of force parameters, is valid for the unstable nuclei.

Thus far, we have arrived at the main conclusion of the present research. However, there are still some important related aspects that should be further discussed. According to Eq. (9), the form factors are connected with the single-nucleon wave functions and the momentum transfer through three reduced matrix elements, $R_L^u(q)$, $R_L^l(q)$, and $R_L^c(q)$, which are the contributions of the upper and lower components of the Dirac four-spinors and the crossed term, respectively. Therefore, the first aspect that we would like to further discuss is how these matrix elements contribute to the form factors and how they change with the neutron number and the momentum transfer. In Fig. 5, we plot the $R_L^u(q)$, $R_L^l(q)$, and $R_L^c(q)$ of the $2s_{1/2}$ state wave functions of ^{25,29,33,37,41,45}P with the NL-SH parameters being adopted. Figure 6 is the same as Fig. 5, but for the $1d_{3/2}$ states of ^{37,41,45}P. Figures 6(a)–6(c)

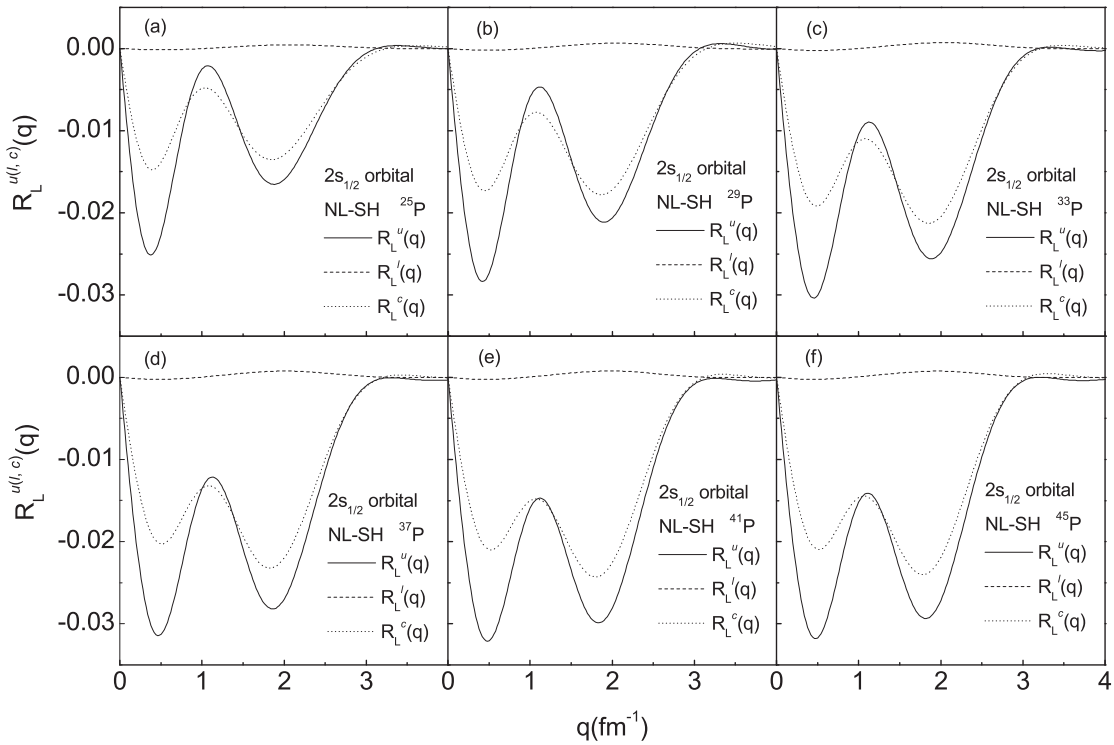

FIG. 5. The contributions of the upper components $R_L^u(q)$ (solid lines), the lower components $R_L^l(q)$ (dashed lines), and the crossed term $R_L^c(q)$ (dotted lines) of the $2s_{1/2}$ wave function.

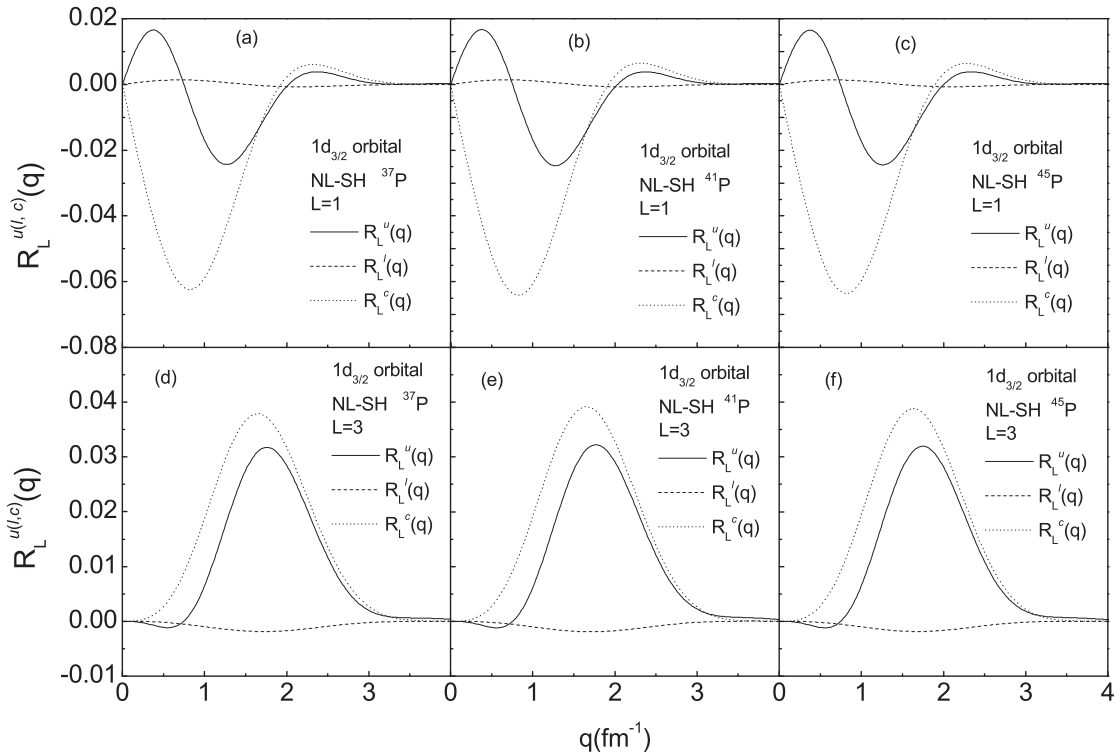

FIG. 6. The same as Fig. 5, but for the $1d_{3/2}$ states of ^{37,41,45}P. The upper [(a)−(c)] and lower [(d)−(f)] panels are the results corresponding to multipoles $L = 1$ and $L = 3$, respectively.

and 6(d)–6(f) are the results corresponding, respectively, to multipoles $L = 1$ and $L = 3$. It can be noted from both figures that, within the momentum transfer region $q = 0$–$3.0\ \mathrm{fm}^{-1}$, the contributions of the upper components $R_L^u(q)$ and the crossed term $R_L^c(q)$ are of the same order of magnitude, whereas the contribution of the lower components $R_L^l(q)$ are much smaller (nearly two orders smaller), so the contribution of the lower components alone to the form factors is very small.

Indeed, the lower components alone contribute very little to the form factors; however, the importance of the lower components in elastic magnetic electron-nucleus scattering can not at all be underestimated. The importance of the lower components is embodied in the contribution of the crossed term, which bears the difference between the relativistic nuclear structure models and nonrelativistic nuclear structure models. In addition, Figs. 5 and 6 also show that the amplitudes of contribution of the upper components of the $2s_{1/2}$ and $1d_{3/2}$ wave functions show only some slight differences, whereas the amplitudes of contribution of the crossed term of the two states show remarkable deviations. For the $2s_{1/2}$ state, the amplitude of the contribution of the crossed term is smaller than that of the upper components, but, in contrast, the amplitude of the contribution of the crossed term is larger than that of the upper components for $1d_{3/2}$. More than that, Figs. 6(a)–6(c) show that the amplitude of the crossed term of $1d_{3/2}$ with multipole $L = 1$ is about 2 times larger than that of the upper components. To know why there exist such deviations, let us make a comparison of the contributions of the lower components of the two states. We take ^{39,43}P as instances. Figure 7 is the plot of the absolute values of the contributions $R_L^l(q)$ of the lower components of the $2s_{1/2}$ and $1d_{3/2}$ single-nucleon wave functions of ^{39,43}P. The figure shows that the contributions of the lower components of $1d_{3/2}$ (dashed and dotted lines) are approximately one order larger than that of the $2s_{1/2}$ state (solid lines) within the momentum transfer regions $q = 0.0$–$1.25\ \mathrm{fm}^{-1}$ for $L = 1$ and $q = 0.5$–$2.25\ \mathrm{fm}^{-1}$ for $L = 3$, respectively. This implies that, compared with the $2s_{1/2}$ state, the lower components of the $1d_{3/2}$ state may undergo an enhancement [58,59], and, as a result, the enhancement has led to the remarkable deviations between $R_L^u(q)$ and $R_L^c(q)$ shown in Fig. 6 and Fig. 5. This reveals that the lower components play a significant role in elastic magnetic electron-nucleus scattering. The enhancement of the lower components of the Dirac four-spinors was first found and studied by J. A. Caballero *et al.* [58,59] when the authors were investigating the role of the lower components in the response functions of the $(e,e'p)$ processes. Their study shows that the lower components play an important role in quasielastic electron scattering [58,59]. The results of our calculation and discussion of elastic magnetic electron-nucleus scattering based on the RMF model agree with and support the conclusion given by these authors.

The second interesting aspect is about the isotopic shifts of the form factors shown in Fig. 3. Why do the form factors shift with an increasing neutron number? The above discussion shows that the single-nucleon form factors are almost completely determined by the contributions of the upper components and the crossed term. Figure 5 shows that for the fixed $2s_{1/2}$ orbital, the contributions of the upper components

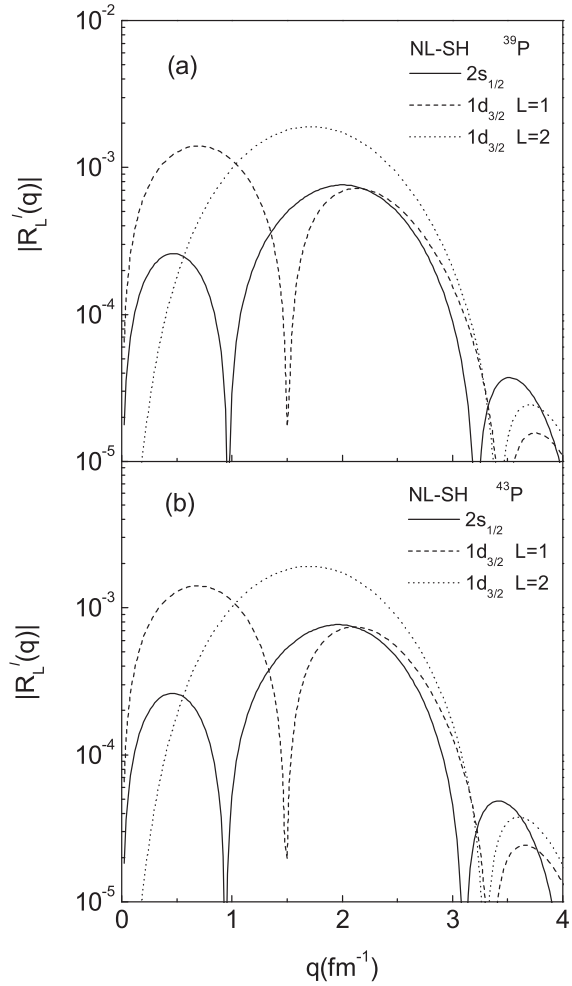

FIG. 7. The contributions of the lower components $R_L^l(q)$ of the $2s_{1/2}$ and $1d_{3/2}$ single-nucleon wave functions of ^{39,43}P.

and the crossed term have the same sign within the momentum transfer region $q = 0$–$3.0\ \mathrm{fm}^{-1}$, and both gradually increase with a decaying speed with the increase of neutron number. The figure also shows that the second peak of both contributions appears to increase more rapidly than the first peak. It is these changes of the two contributions that have led to the isotopic shifts shown in Fig. 3. To consider the problem more deeply in view of the mean-field model, the fundamental reasons for the isotopic shifts, as well as for the changes of the contributions of the upper components and the crossed term, should be the change of the mean field caused by the increase of the neutron number. However, since the nucleons, the mesons, and the photons are coupled together, the field corresponding to each kind of meson and photon will change with the increase of the neutron number. Therefore, the shifts should be the combined effect of the changes of the σ, ω, ρ, and Coulomb fields. Nevertheless, we expect that, among the four potential fields, there may be one or two directly related with the change of neutron number, whose change plays the most important role. Detailed analysis of the four field potentials shows that the sum of the potentials of the attractive σ field, the repulsive ω field, and the Coulomb field only shows a

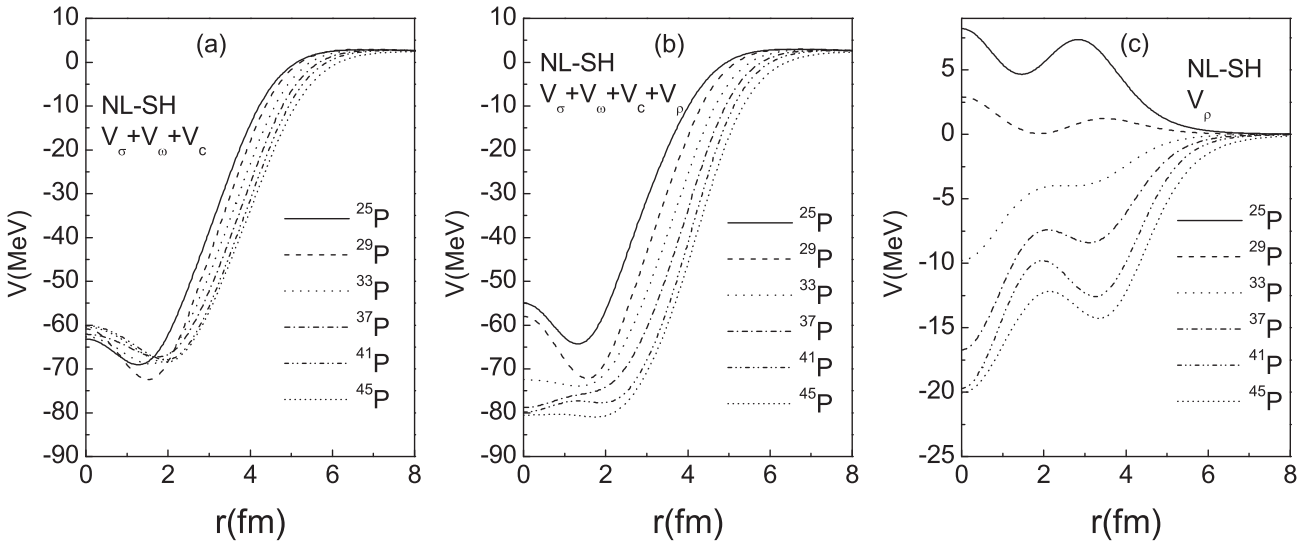

FIG. 8. The variations of the potentials $V_\sigma + V_\omega + V_c$ (a), $V_\sigma + V_\omega + V_c + V_\rho$ (b), and V_ρ (c) with the increase of neutron number, where V_σ, V_ω, V_c, and V_ρ denote the potentials of the σ, ω, Coulomb, and ρ fields, respectively.

very slight change with the increase of the neutron number. Figure 8(a) shows that both the depth and width of the potential well vary within only a very small range for an increase of 20 neutrons. The range of variation of the depth is less than 6 MeV and that of the width is within 1 fm. However, after the potential of the ρ field is taken into account, the total potential shows a significant variation [see Fig. 8(b)]. The depth of the total potential well varies within a range as large as 25 MeV, and the variation range of the width is also nearly doubled. In addition, the crossings of the potential curves at the bottoms of the potential wells shown in Fig. 8(a) also disappeared in Fig. 8(b). This indicates that the change of the ρ field plays the most significant role in producing the isotopic shifts. This conclusion is just what was expected, since the source of the ρ field is nothing but the difference between the neutron and proton densities. For comparison, the variation of the ρ field potential is also plotted in Fig. 8(c). It is seen that the changes of V_ρ turn from very "violent" to very "mild" as the neutron number increases from $N = 10$ to $N = 30$. This also explains why the isotopic shifts become nonsignificant for the very neutron-rich phosphorus isotopes.

The third aspect that we would like to discuss is about the changes of the form factors obtained with the three force parameter sets (NL-SH, TM2, and NL3) for a fixed nucleon orbital of the same isotope. Figures 2–4 all show that the form factors from the three parameter sets for the fixed $2s_{1/2}$ or $1d_{3/2}$ orbital have some noticeable changes. According to the RMF nuclear structure theory, the changes of the form factors should result from the variations of the mean field generated with the three parameter sets. To find which of the four nuclear field potentials (the σ, ω, ρ, and Coulomb fields) are mainly responsible for these changes, we need to make a detailed comparison between the results generated with the NL-SH, TM2, and NL3 parameters for each field potential. Here we exemplify it with the results of ^{31}P. In Fig. 9(a), we plot the results of the σ and ω field potentials (for the convenience of comparison, $-V_\sigma$ is plotted in the figure). Figures 9(b) and 9(c) are the results of the ρ and Coulomb fields, respectively. The figures show that the results from the three parameter sets for each field potential all, to some extent, have deviations from each other. For instance, the deviation of the results of V_σ between NL-SH and NL3 at $r = 0.0$ fm is about 58.0 MeV and that between NL-SH and TM2 around $r = 2.0$ fm is about 40.0 MeV; for V_ρ and V_c, the largest deviations among the three results, which occur at the center, are at most 1.0 and 0.5 MeV, respectively. In addition, noticeable deviations between the results of V_ρ and between those of V_c shown in Figs. 9(b) and 9(c) occur approximately between $r = 0.0$ fm and $r = 3.0$ fm, while those of V_σ and V_ω shown in Fig. 9(a) appear within a much larger spatial region, from $r = 0.0$ fm to at least $r = 8.0$ fm on the same scale as those of V_ρ and V_c. Therefore, one can see that the absolute deviations between the results of V_σ and between those of V_ω are much larger than those of V_ρ and V_c. In Fig. 9(d), we present the results of $V_\sigma + V_\omega$, which accounts for the main part of the total mean-field potential. In Figs. 9(e) and 9(f), the results of $V_\sigma + V_\omega + V_\rho$ and $V_\sigma + V_\omega + V_\rho + V_c$ are also given for comparison. Figure 9(d) shows that the deviations between the results of V_σ and between those of V_ω are largely canceled after the results of V_σ and V_ω from the same parameter sets are added up; only a small proportion of the deviations can pass down to the resultants. Even so, the deviations between the three resultants in Fig. 9(d) are still much larger than those between the results of V_ρ shown in Fig. 9(b) and those between the results of V_c shown in Fig. 9(c). The evolution of the resultant potentials from Fig. 9(d) through Figs. 9(e) to 9(f) shows that the changes of the field potentials V_ρ and V_c with NL-SH, NL3, and TM2 do not make much difference to the total mean-field potential; the changes of the total potential with NL-SH, NL3, and TM2 are mainly inherited from the variations of V_σ and V_ω. Therefore, it can be concluded that it is the variations of V_σ and V_ω obtained with different parameter sets whose combined effect are mainly responsible for the changes of the total potential and thus responsible for the changes of the form

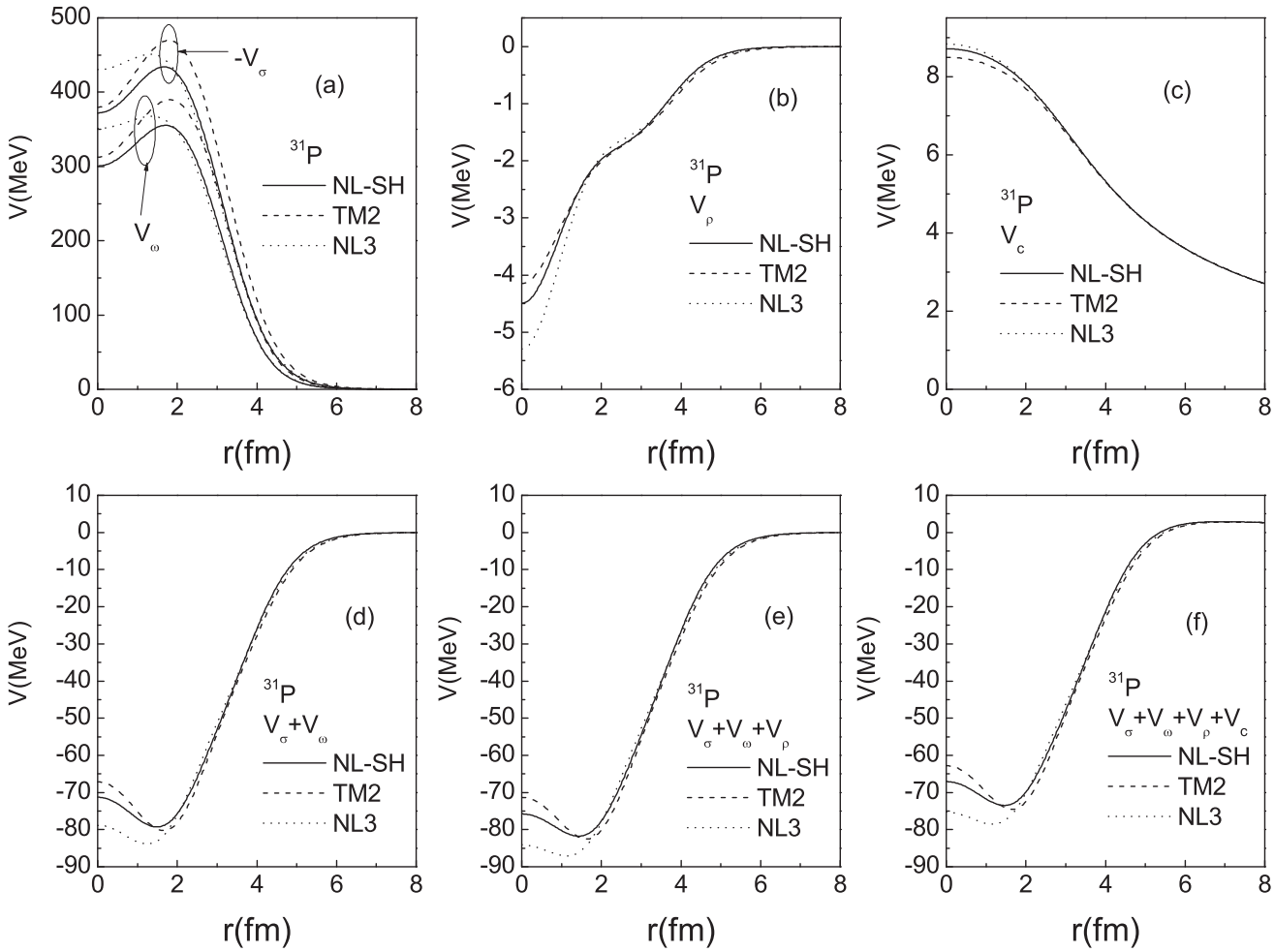

FIG. 9. The variations of the field potentials V_σ, V_ω, V_ρ, V_c, $V_\sigma + V_\omega$, $V_\sigma + V_\omega + V_\rho$, and $V_\sigma + V_\omega + V_\rho + V_c$ obtained with NL-SH, TM2, and NL3 parameter sets for ^{31}P. In (a), the three curves circled by the upper small ellipse correspond to $-V_\sigma$ and those by the lower ellipse correspond to V_ω.

factors obtained with the NL-SH, TM2, and NL3 parameter sets.

Finally, a few remarks should be made on the method and results of the present paper. As a first attempt, we investigated the spins and parities of the odd-A P isotopes $^{25-47}$P by combining the relativistic elastic magnetic electron-nucleus scattering theory with the RMF nuclear structure model. Actually, nuclei in the considered region are known to be deformed, so a more reasonable and realistic method should be one that can take into account the deformation of the nuclei. From this point of view, there should exist much room for the method and results to be further improved. As a matter of fact, good work in calculating the elastic magnetic form factors based on deformed nuclear structure models have been done by other authors [60], and the spectroscopy factors used in the present paper can also be produced directly from the deformed model for spin $\frac{1}{2}$ ground-state nuclei [61–63]. In Ref. [60], E. Graca *et al.* introduced a deformed model approach to calculating the elastic magnetic form factors of odd-A nuclei. In this method, a relation of dependence of the elastic magnetic form factors on the deformation parameter, which bears much physical interest, are built such that the spherical single-nucleon form factors can be naturally brought down to agree with the experimental data by adjusting the deformation parameter to reproduce the experimental nuclear magnetic moments. With this method, the elastic magnetic form factors of ^{29}Si can be better reproduced. Therefore, we expect that with this method more accurate elastic magnetic form factors can be obtained for the considered isotopes $^{25-47}$P.

IV. SUMMARY

With the combination of the RMF model and the elastic magnetic electron-scattering theory in the relativistic frame, we have theoretically investigated the spins and parities of the odd-A isotopes $^{25-47}$P and explored the feasibility of experimentally studying the s-d level inversion and spins and parities of $^{37-47}$P with elastic magnetic electron nucleus scattering. The RMF model calculations show that for the isotopes $^{27-35}$P, whose spins and parities have been determined by experiments, the results given by the NL-SH, TM2, and NL3 parameters all agree with the experimental ones [1]. For

$^{37-47}$P, whose spins and parities have not been determined, the RMF model results show that the order of the $2s_{1/2}$ and $1d_{3/2}$ single proton levels may be inverted by the neutron excess and, consequently, two possible spin-parity values $\frac{1}{2}^+$ and $\frac{3}{2}^+$ are obtained with the three parameter sets. For ^{37,39}P, the results may be either $\frac{1}{2}^+$, which agrees with those given by the NUBASE2012 data table, or $\frac{3}{2}^+$; for $^{41-45}$P, the results are $\frac{3}{2}^+$, which differs from those given by NUBASE2012; for ^{47}P the results are $\frac{3}{2}^+$, the same as that given by NUBASE2012. The calculations with the elastic magnetic electron-scattering theory show that the form factors of $^{37-47}$P between the two different states of motion of the single valence proton, $2s_{1/2}$ and $1d_{3/2}$, significantly differ. The results imply that elastic magnetic electron scattering can be a possible method for experimentally probing the possible *s*-*d* level inversion and the spins and parities of $^{37-47}$P. The results can also be used for testing the validity of the RMF model for describing unstable nuclei.

We also made a discussion on the contributions of the upper components and lower components of the single nucleon-wave functions and that of the crossed term. It was found that the contributions of the lower components alone can be neglected; nevertheless, the importance of the lower components cannot be underestimated. The lower components may undergo an enhancement in elastic magnetic electron-nucleus scattering, and in this case, the contribution of the crossed term to the form factors can be larger than that of the upper components. This shows that the lower components of the Dirac four-spinors play an important role in elastic magnetic electron-nucleus scattering. The result agrees with and supports the conclusion given in the literature [58,59].

In addition, the isotopic shifts of the elastic magnetic form factors and the changes of the form factors for a fixed orbital of the same nucleus obtained with different parameter sets (NL-SH, TM2, and NL3) were also discussed. It was found that the isotopic shifts of the elastic magnetic form factors are mainly out of the change of the ρ field with the increase of neutron number and that the changes of the form factors obtained with different parameter sets are mainly due to the change of the σ and ω fields.

ACKNOWLEDGMENTS

This work was supported by the National Natural Science Foundation of China (Grants No. 11275138, No. 10675090, No. 10975072, and No. 1134712), by the Tianjin Research Program of Application Foundation and Advanced Technology (Grant No. 11JCYBJC26900), and by the Research Fund of Tianjin University of Technology and Education (Grant No. KJYB11-3).

[1] G. Audi, F. G. Kondev, M. Wang *et al.*, Chin. Phys. C **36**, 1157 (2012).
[2] T. W. Donnelly and I. Sick, Rev. Mod. Phys. **56**, 461 (1984).
[3] R. Hofstadter, Rev. Mod. Phys. **28**, 214 (1956).
[4] R. Hofstadter, Annu. Rev. Nucl. Sci. **7**, 231 (1957).
[5] R. Hofstadter, *Nodel Lecture 1961, Nobel Lectures—Physics* (Elsevier, Amsterdam, 1964).
[6] H. Überall, *Electron Scattering from Complex Nuclei* (Academic Press, New York, 1971).
[7] J. D. Walecka, *Electron Scattering for Nuclear and Nucleon Structure* (Cambridge University Press, Cambridge, 2001).
[8] M. V. Hynes *et al.*, Phys. Rev. Lett. **42**, 1444 (1979).
[9] N. Kalantar-Nayestanaki *et al.*, Phys. Rev. Lett. **60**, 1707 (1988).
[10] S. Platchkov *et al.*, Phys. Rev. Lett. **61**, 1465 (1988).
[11] H. Baghaei *et al.*, Phys. Rev. C **42**, 2358 (1990).
[12] J. Heisenberg and H. P. Blok, Ann. Rev. Nucl. Part. Sci. **33**, 569 (1983).
[13] T. Suda, K. Maruyama, and I. Tanihata, RIKEN Accel. Prog. Rep. **34**, 49 (2000).
[14] M. Wakasugi, T. Suda, and Y. Yano, Nucl. Instrum. Methods **A532**, 216 (2004).
[15] T. Suda and M. Wakasugi, Prog. Part. Nucl. Phys. **55**, 417 (2005).
[16] T. Motobayashi, in *Recent Achievements and Perspectives in Nuclear Physics: Proceedings of the Vth Italy-Japan Symposium*, edited by G. La Rana, C. Signorini, and S. Shimoura (World Scientific, Hackensack, NJ, 2005), p. 563.
[17] T. Suda, M. Wakasugi, T. Emotto *et al.*, Phys. Rev. Lett. **102**, 102501 (2009).
[18] M. Wakasugi, T. Emotto *et al.*, Eur. Phys. J. A **42**, 453 (2009).
[19] A. N. Antonov, M. K. Gaidarov, M. V. Ivanov *et al.*, Nucl. Instrum. Methods A **637**, 60 (2011).
[20] S. Abrahamyan, Z. Ahmed, H. Albataineh *et al.*, Phys. Rev. Lett. **108**, 112502 (2012).
[21] M. M. Dalton, Phys. Part. Nucl. **45**, 317 (2014).
[22] C. J. Horowitz, Z. Ahmed, C.-M. Jen *et al.*, Phys. Rev. C **85**, 032501(R) (2012).
[23] K. S. Jassim, A. A. Al-Sammarrae, F. I. Sharrad, and H. A. Kassim, Phys. Rev. C **89**, 014304 (2014).
[24] I. Sick and D. Trautmann, Phys. Rev. C **89**, 012201(R) (2014).
[25] X. Roca-Maza, M. Centelles, F. Salvat, and X. Viñas, Phys. Rev. C **78**, 044332 (2008); **87**, 014304 (2013).
[26] E. Garrido and E. Moya de Guerra, Nucl. Phys. A **650**, 387 (1999); Phys. Lett. B **488**, 68 (2000).
[27] A. N. Antonov, D. N. Kadrev, M. K. Gaidarov, E. Moya de Guerra, P. Sarriguren, J. M. Udias, V. K. Lukyanov, E. V. Zemlyanaya, and G. Z. Krumova, Phys. Rev. C **72**, 044307 (2005).
[28] P. Sarriguren, M. K. Gaidarov, E. M. de Guerra, and A. N. Antonov, Phys. Rev. C **76**, 044322 (2007).
[29] S. Karataglidis and K. Amos, Phys. Lett. B **650**, 148 (2007).
[30] C. A. Bertulani, J. Phys. G **34**, 315 (2007).
[31] S. F. Ban, C. J. Horowitz, and R. Michaels, J. Phys. G **39**, 15104 (2012).
[32] J. Liu, Z. Ren, T. Dong, and Z. Sheng, Phys. Rev. C **84**, 064305 (2011).
[33] A. Meucci, M. Vorabbi, C. Giusti, F. D. Pacati, and P. Finelli, Phys. Rev. C **87**, 054620 (2013).
[34] H. Miessen, H. Rothhaas, G. Lührs, G. A. Peterson *et al.*, Nucl. Phys. A **430**, 189 (1984).
[35] J. Wesseling, C. W. de Jager, L. Lapikás, H. de Vries, L. W. Fagg, M. N. Harakeh, N. Kalantar-Nayestanaki, R. A. Lindgren,

E. Moya de Guerra, and P. Sarriguren, Phys. Rev. C **55**, 2773 (1997).
[36] H. de Vries, C. W. de Jager, and C. de Vries, At. Data Nucl. Data Tables **36**, 495 (1987).
[37] P. Raghavan, At. Data Nucl. Data Tables **42**, 189 (1989).
[38] B. D. Serot and J. D. Walecka, *Advances in Nuclear Physics*, edited by J. W. Negele and E. Vogt (Plenum, New York, 1986), Vol. 16, p. 1.
[39] J. D. Walecka, Ann. Phys. (NY) **83**, 491 (1974).
[40] J. D. Walecka, Phys. Lett. B **94**, 293 (1980).
[41] Y. K. Gambhir, P. Ring, and A. Thimet, Ann. Phys. (NY) **198**, 132 (1990).
[42] C. J. Horowitz and B. D. Serot, Nucl. Phys. A **368**, 503 (1981).
[43] M. M. Sharma, M. A. Nagarajan, and P. Ring, Phys. Lett. B **312**, 377 (1993).
[44] Z. Ma, H. Shi, and B. Chen, Phys. Rev. C **50**, 3170 (1994).
[45] G. A. Lalazissis, J. König, and P. Ring, Phys. Rev. C **55**, 540 (1997).
[46] Z. Ren, W. Mittig, and F. Sarazin, Nucl. Phys. A **652**, 250 (1999).
[47] Z. Ren, W. Mittig, B. Chen, and Z. Ma, Phys. Rev. C **52**, R20 (1995).
[48] Y. Sugahara and H. Toki, Nucl. Phys. A **579**, 557 (1994).
[49] B. G. Todd-Rutel and J. Piekarewicz, Phys. Rev. Lett. **95**, 122501 (2005).
[50] J. D. Bjorken and S. D. Drell, *Relativistic Quantum Mechanics* (McGraw–Hill, New York, 1964).
[51] T. de Forest and J. D. Walecka, Adv. Phys. **15**, 1 (1966).
[52] T. W. Donnelly and J. D. Walecka, Nucl. Phys. A **201**, 81 (1973).
[53] A. R. Edmonds, *Angular Momentum in Quantum Mechanics* (Princeton University Press, Princeton, NJ, 1960).
[54] E. J. Kim, Phys. Lett. B **174**, 233 (1986).
[55] B. D. Serot, Phys. Lett. B **107**, 263 (1981).
[56] R. S. Willey, Nucl. Phys. **40**, 529 (1963).
[57] T. Dong, Z. Ren, and Y. Guo, Phys. Rev. C **76**, 054602 (2007).
[58] J. A. Caballero, T. W. Donnelly, E. Moya de Guerra, and J. M. Udias, Nucl. Phys. A **643**, 189 (1998).
[59] J. E. Amaro, J. A. Caballero, T. W. Donnelly, and E. Moya de Guerra, Nucl. Phys. A **611**, 163 (1996).
[60] E. Graca, P. Sarriguren, D. Berdichevsky *et al.*, Nucl. Phys. A **483**, 77 (1988).
[61] E. Moya de Guerra and S. Kowalski, Phys. Rev. C **20**, 357 (1979).
[62] E. Moya de Guerra and S. Kowalski, Phys. Rev. C **22**, 1308 (1980).
[63] P. Sarriguren, E. Moya de Guerra, R. Nojarov, and A. Faessler, J. Phys. G **20**, 315 (1994).